THE JOURNAL OF PHYSICAL CHEMISTRY A LETTERS

2008, *112,* 4715–4718
Published on Web 05/07/2008

Bromide Control, Bifurcation and Activation in the Belousov−Zhabotinsky Reaction

Harold M. Hastings,*,[†] Sabrina G. Sobel,[†] Richard J. Field,[‡] Dominick Bongiovi,[†] Brianna Burke,[†] Daniel Richford,[†] Kara Finzel,[†] and Melissa Garuthara[†]

Department of Chemistry and Department of Physics and Astronomy, Hofstra University, Hempstead, New York 11549-1510, and Department of Chemistry, The University of Montana, Missoula, Montana 59812

Received: March 4, 2008; Revised Manuscript Received: April 18, 2008

The unstirred, ferroin ($Fe(phen)_3^{2+}$) catalyzed Belousov−Zhabotinsky (BZ) reaction is the prototype oscillatory chemical system. Reaction media with added Br^- appear red (reduced, low [$Fe(phen)_3^{3+}$]) during an induction period of several minutes, followed by the "spontaneous" formation of "pacemaker" sites, which oscillate between a blue, oxidized state (high [$Fe(phen)_3^{3+}$]) and the red, reduced state and generate target patterns of concentric, outwardly moving waves of oxidation (blue). Auto-oscillatory behavior is also seen in the Oregonator model of Field, Kõrös and Noyes (FKN), a robust, reduced model that captures qualitative BZ kinetics in the auto-oscillatory regime. However, the Oregonator model predicts a blue (oxidized) induction phase. Here we develop a generalized Oregonator-like model with *no* explicit bifurcation parameter that yields the observed transition from a red initial state to oscillatory dynamics, and displays a new bifurcation mechanism not seen in the original Oregonator.

The unstirred, ferroin ($Fe(phen)_3^{2+}$) catalyzed Belousov−Zhabotinsky (BZ) reaction[1−8] is the prototype oscillatory chemical system. In reaction mixtures in a Petri dish, with Br^- initially added for production of bromomalonic acid, one sees the "spontaneous" formation of target patterns of concentric, outwardly moving waves of oxidation (blue, high-ferriin ([$Fe(phen)_3^{3+}$])) in a red/reduced/low-ferriin reaction medium, following an initiation period of several minutes in a red steady state.

The Field, Kõrös and Noyes (FKN) Oregonator model,[5,6] a robust, reduced model for BZ kinetics, also displays oscillatory (red/blue) dynamics. However, the standard Oregonator bifurcation scenario cannot yield the observed transition from a red steady state to oscillatory dynamics. In prior work, we showed[9] how spontaneous pattern formation might follow from slow passage[10] through a bifurcation in Oregonator dynamics. We explained[11] the initial red state by including Br^- production from FKN reaction R8, not in the original Oregonator.

Here we show that FKN dynamics combined with an explicit model for the enolization of malonic acid (MA) and bromination of the enol form of MA via reaction FKN 8 yields the observed initial red steady state in the presence of initial Br^-. This yields a generalized Oregonator-like model with a stoichiometric factor f fixed at 2, whose dynamics evolves from a red steady state to Oregonator-like oscillatory dynamics. Thus the stoichiometric factor f no longer plays the role of an explicit time-varying bifurcation parameter. Finally, the rate of Br^- production, which includes Br^- produced by FKN 8 as well as that produced in Oregonator dynamics, serves as a control parameter, reproducing the observed transition from a red, reduced, high [Br^-] state to oscillatory dynamics.

The Oregonator is a system of three differential equations that captures essentially all of the main dynamical features of the BZ reaction:

$$\mathrm{d}x/\mathrm{d}t = k_3[\mathrm{BrO_3}^-][\mathrm{H}^+]^2 y - k_2[\mathrm{H}^+]xy + k_5[\mathrm{BrO_3}^-][\mathrm{H}^+]x - k_4x^2$$

$$\mathrm{d}y/\mathrm{d}t = -k_3[\mathrm{BrO_3}][\mathrm{H}^+]^2 y - k_2[\mathrm{H}^+]xy + (f/2)k_c[\mathrm{MA}]_0 z$$

$$\mathrm{d}z/\mathrm{d}t = 2k_5[\mathrm{BrO_3}^-][\mathrm{H}^+]x - k_c[\mathrm{MA}]_0 z \qquad (1)$$

Here $x = [HBrO_2]$, $y = [Br^-]$, $z = 2[M^{n+1}]$, the oxidized form of the catalyst (e.g., $Fe(phen)_3^{3+}$ for ferroin/ferriin as catalyst, Ce^{4+} for Ce^{3+}/Ce^{4+}as catalyst, Mn^{3+} for $Mn^{2+/3+}$ as catalyst). $[H^+]$, $[BrO_3]$ and $[MA]_0$ are regarded as parameters and do not evolve. The "stoichiometric factor" f parametrizes the following simplified model for Br^- produced by reduction of the oxidized catalyst M^{n+1} and corresponds roughly to the ratio [BrMA]/[MA]:

$$\text{FKN 9, 10:} \qquad 2\mathrm{M}^{n+1} + \mathrm{MA} + \mathrm{BrMA} \rightarrow f\mathrm{Br}^- + 2\mathrm{M}^n + \text{other products} \quad (2)$$

where some MA is brominated to form bromomalonic acid, denoted BrMA. Oregonator dynamics depends upon a difference in time scales between fast dynamics of the autocatalytic species $x = [HBrO_2]$ and slow dynamics of the catalyst $z = 2[M^{n+1}]$. Reduction of the catalyst in eq 2 produces the inhibitory species $y = [Br^-]$ at a rate parametrized by f. Thus f serves as a bifurcation parameter, with a "low-f " Hopf bifurcation at $f \approx 1/2$ and a "high-f " reverse Hopf bifurcation at $f \approx 1 + 2^{1/2}$. At low f, Br^- production is insufficient to stop autocatalysis and

---

* Corresponding author. E-mail: Harold.Hastings@Hofstra.edu.
[†] Hofstra University.
[‡] The University of Montana.

10.1021/jp8019073 CCC: $40.75

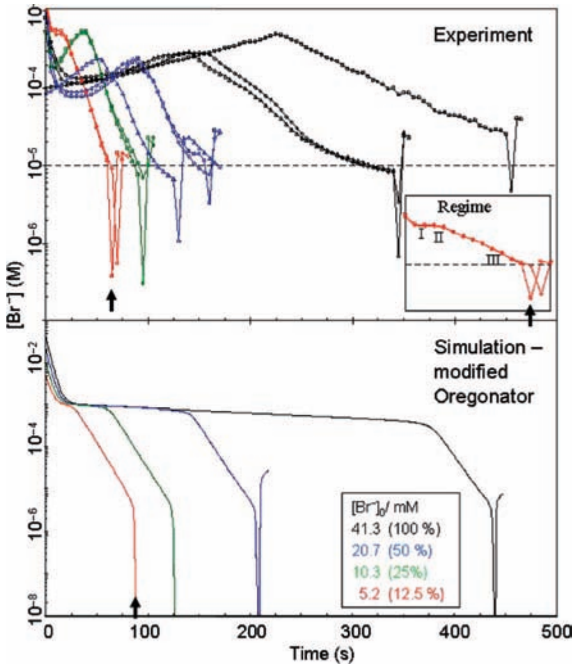

Figure 1. Experimental (top) and simulation (bottom) dynamics of $[Br^-]$ in the ferroin-catalyzed BZ reaction. The onset of activation is marked by a sharp decrease in $[Br^-]$ (↑). The inset illustrates the three dynamical regimes: (I) relatively rapid decrease of $[Br^-]$ as initial $[Br^-]$ is consumed; (II) constant or increasing $[Br^-]$ as Br^- is generated in bromination of MA; (III) slow decrease of $[Br^-]$ followed by activation, autocatalysis of $[HBrO_2]$ and a very sharp decrease in $[Br^-]$ (↑), seen here in an experimental run with $[Br^-]_0 = 0.0051625$ M.

oxidation of the catalyst, yielding a blue/oxidized steady state; at high *f*, Br^- production stops autocatalysis and thus oxidation of the catalyst, yielding a red/reduced steady state. At intermediate *f* (between $\sim^1/_2$ and $\sim 1 + 2^{1/2}$) one sees large amplitude limit cycle oscillations between the blue and red states. Although eq 2 implies $f \leq 2$, the formation of dibromomalonic acid and other sources of Br^- may yield higher *effective* values of *f*, sufficient to yield the observed red state.

The evolution of *f* is governed by the bromination of MA to form BrMA, for example. via

$$\text{FKN 8:} \qquad \mathrm{MA + Br_2 \rightarrow BrMA + H^+ + Br^-} \qquad (3)$$

At time $t = 0$, there are no brominated forms of MA, and thus $f = 0$. Moreover, *f* increases with bromination of MA to form BrMA. By itself, the resulting *increase* in *f* can yield the low-*f* bifurcation from a blue steady state to oscillatory behavior, but *not* the high-*f* *reverse* bifurcation from the observed red state.

In addition, unlike Mn^{3+} and Ce^{4+}, ferriin cannot oxidize MA[12,13] due to its relatively low redox potential.[14] Thus reaction 2 becomes

$$\mathrm{2M^{n+1} + 2BrMA \rightarrow 2Br^- + 2M^n + other\ products} \qquad (4)$$

making $f = 2$ very shortly after the start, yielding oscillatory dynamics.

However, reaction 3 also provides a source of Br^- from bromination of MA. This yields a high *effective* *f* ($>1 + 2^{1/2}$) and thus drives the system to the red steady state observed shortly after reagents are mixed. Oscillations begin after Br_2, produced early in the BZ reaction, is consumed and Br^- production from reaction 3 essentially ceases. This yields a generalized high-*f* bifurcation in Oregonator-like dynamics, explaining the observed oxidation state at initiation, followed by a transition to oscillatory dynamics with $f = 2$.

Our starting point is an experimental investigation of Br^- dynamics. As in our previous work,[10] we used a modified Shakhashiri[8] recipe with the concentration of BrO_3^- stock solution reduced to 0.40 M (final $[BrO_3^-] = 0.25$ M) because of low solubility of $KBrO_3$. Other final concentrations were $[H_2SO_4] = 0.30$ M, $[MA] = 0.10$ M, $[ferroin] = 0.00052$ M. $[KBr]_0$ was varied from 0.0413 M (as in Shakhashiri) to $^1/_8$ of 0.0413 M = 0.00516 M to explore the effects of initial $[Br^-]$. $[Br^-]$ was measured with a Metrohm 781 pH/Ion meter with a Metrohm bromide ISE and an Ag/AgCl reference electrode. Reactions were run in a 150 mL beaker, and stirred to provide a homogeneous medium; without stirring, oscillations always began at the edge of the electrode. Data were captured by Vesuv 3.0 software (Metrohm 2005).

Results are shown in the top panel of Figure 1. The duration of the induction period before the first activation (indicated by a sharp decrease in $[Br^-]$) increases with increasing initial $[Br^-]$, and the induction period consists of three distinct dynamical regimes:

(I) an initial relatively rapid decrease in $[Br^-]$ to $\sim 10^{-4}$ M,

(II) an increase in $[Br^-]$ (for $[Br^-] > 0.01$ M), or a significantly slower decrease in $[Br^-]$ for lower $[Br^-]_0$, and finally,

(III) a relatively slow decrease in $[Br^-]$ to $\sim 10^{-5}$ M, followed by a sharp decrease (activation).

We then combined FKN kinetics with bromination of MA and consequent Br^- release (reaction FKN 8, above) rate limited by enolization of MA.[5,15] Here is the resulting skeleton model. Following Scott,[7] "classical" FKN kinetics of an oscillatory ferroin/ferriin catalyzed BZ reaction is a cycle of three processes:

Process A: removal of the inhibitory species Br^-. The Oregonator includes FKN 2 and FKN 3; we also include FKN 1, an important source of Br_2.

$$\mathrm{BrO_3^- + Br^- + 2H^+ \rightarrow HBrO_2 + HOBr} \qquad \text{(FKN3)}$$

$$\mathrm{HBrO_2 + Br^- + H^+ \rightarrow 2HOBr} \qquad \text{(FKN2)}$$

$$\mathrm{HOBr + Br^- + H^+ \rightarrow Br_2 + H_2O} \qquad \text{(FKN1)}$$

Process B: autocatalytic production of $HBrO_2$. As in the Oregonator, FKN 5 and FKN 6 are combined, with FKN 5 the rate-limiting step.

$$\mathrm{BrO_3^- + HBrO_2 + H^+ \rightarrow 2BrO_2^{\bullet} + H_2O} \qquad \text{(FKN5)}$$

$$\mathrm{BrO_2^{\bullet} + Fe(phen)_3^{2+} + H^+ \rightarrow HBrO_2 + Fe(phen)_3^{3+}} \qquad \text{(FKN6)}$$

Autocatalysis is limited by the disproportionation

$$\mathrm{2HBrO_2 \rightarrow BrO_3^- + HOBr + H^+} \qquad \text{(FKN4)}$$

allowing process C below to remove $HBrO_2$ and reset the clock.

Process C: reduction of the oxidized catalyst, regeneration of Br^- and removal of $HBrO_2$

$$\mathrm{Fe(phen)_3^{3+} + BrMA \rightarrow Fe(phen)_3^{2+} + Br^- + organic\ products} \qquad \text{(FKN10)}$$

For catalysts such as Mn^{3+} and Ce^{4+}, which can oxidize MA, process C also includes its oxidation, leading to eq 2 above, including the stoichiometric and potential bifurcation factor *f*.

Finally, Br_2 produced in reaction FKN 1 brominates the enol form of MA via the reactions:[5,15]

$$\text{MA/keto} \leftrightarrows \text{MA/enol} \qquad (5)$$

$$\text{MA/enol} + Br_2 \rightarrow \text{BrMA} + H^+ + Br^- \qquad (\text{FKN8})$$

where the enolization rates $k_{enol} = 0.0026\ s^{-1}$ and the inverse rate $k_{-enol} = 180\ s^{-1}$ are taken from ref 15. Other references, e.g., refs 5 and 16, give significantly lower k_{enol} that delay simulated activations well beyond observed experimental activations.

Process A combined with bromination of MA and consequent Br^- production might produce much of the observed Br^- dynamics. First process A causes a rapid decrease in $[Br^-]$ (regime I in Figure 1: experimental) and increase in $[Br_2]$. Because FKN 2 and FKN 3 are first order in $[Br^-]$, the rate of $[Br^-]$ consumption itself decreases until a balance is reached with Br^- production in the enolization-limited bromination of MA (eq 3, FKN 8). At this point, $[Br^-]$ remains constant (compare with regime II) until essentially all MA is brominated to form BrMA. Once bromination of MA is largely complete, $[Br^-]$ production from this process (eq 3, FKN 8) largely ceases. Process A then regains control and $[Br^-]$ again decreases (compare with regime III). An activation is generated when $[Br^-]$ falls so low that control passes from process A to process B: autocatalysis of $[HBrO_2]$.[7]

To verify this hypothesis, we integrated the above FKN model with Mathematica, with all rate constants assigned standard values.[5,6,13] Simulation results (bottom panel of Figure 1) were similar to experiment with three differences:

(a) $[Br^-]$ remains relatively constant during regime II in simulations for all $[Br^-]_0$, whereas $[Br^-]$ increased in regime II in experiments at all but the lowest $[Br^-]_0$. This may be an oxygen effect[17–22] resulting from stirring used to prevent spatial heterogeneity due to the Br^- electrode.

(b) The duration of the induction period was somewhat larger.

(c) Simulations showed a faster $[Br^-]$ decrease in regime III.

Simulations also showed how net Br^- production outside Oregonator kinetics (FKN 1, FKN 8) can produce the observed red steady state and subsequent activation directly from this state. Figure 2 illustrates this process with $[Br^-]_0 = 0.051625$ M). Regularization was required to integrate through the onset of activation (arrow); there was a minimal effect (<0.2 s) on the activation time. (We reduced the reaction rate k_1 (at relatively large $[Br^-]$) from 8×10^9 to $8 \times 10^9/(10^{-5} + [Br^-]/M)\ M^{-2}\ s^{-1}$. The effect upon dynamics was negligible.) This regularization is not needed at higher $[Br^-]_0$.

Because FKN 8 is first order in $[Br_2]$, resulting Br^- production closely tracks $[Br_2]$. In our simulation, $[Br_2]$ increased to a relatively constant level ($\sim 10^{-3}$ M) after 5 s and remained near that level for 15 s. The increased Br^- production outside of Oregonator dynamics for the first 20 s produced the relatively constant $[Br^-]$ observed in regime II. In Regime III ($t \approx 25-85$ s), $[Br^-]$ and thus non-Oregonator Br^- production decreased and process A took over control. Activation (↑) followed at $t \approx 90$ s.

The transition from a high $[Br^-]$ state to oscillatory dynamics at the end of regime III can be interpreted as a generalized high-f reverse bifurcation. If outside Br^- production exceeds $\sim 2 \times 10^{-6}\ M\ s^{-1}$, the Oregonator with $f = 2$ displays a red steady state in contrast to the usual oscillatory dynamics. We may informally regard this as an increase in the effective stoichiometric factor. The observed decrease in outside Br^- production corresponds to a *decrease* in the effective f, and a transition from a red steady state to Oregonator-like oscillatory dynamics as observed at the "classical" high f bifurcation.

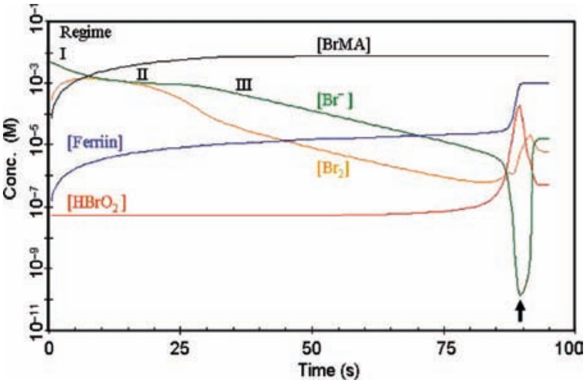

Figure 2. Br^- control in our generalized Oregonator model, with $[Br^-]_0 = 0.051625$ M. Activation (↑) occurs at the end of regime III when bromination of MA by Br_2 is essentially completed, Br^- production from this process (FKN 8) essentially ceases and $[Br^-]$ falls below a critical level of $\sim 10^{-5}$ M. Similar kinetics is observed for other values of $[Br^-]_0$ shown in Figure 1.

The waiting time before activation increased and the period of oscillations decreased as $[Br^-]_0$ increased from 0.0025 to 0.0413 M. We did not observe oscillations outside this range.

In conclusion, a generalized Oregonator with no formal bifurcation parameter and no tuned parameters reproduced the major qualitative features and time scales of the "spontaneous" onset of activations in the BZ reaction. A further understanding of bromine dynamics, especially bromination of MA as a concerted process, formation of dibromomalonic acid, oxygen effects, reversibility of FKN 1[5] and possible additional Br^- production from daughter products in FKN 8 will be required to better simulate observed Br^- dynamics. In particular, activations in simulations of the related reaction with MA replaced by methylmalonic acid (MMA) occur much slower than activations in analogous experimental systems. The time scale for the enolization-limited reaction FKN 8 depends on the enolization rate of the organic acid. Because Br^- production in FKN 8 must be essentially complete before activation, the enolization rate of MMA, $\sim 1/100$ that of MA[23] in the absence of concerted dynamics, significantly delays activation.

Acknowledgment. We acknowledge partial support from NSF CHE-0515691.

References and Notes

(1) Activations of Chemical Excitable Media. 3. Part 1: Hastings, H. M.; Field, R. J.; Sobel, S. G. *J. Chem. Phys.* **2003**, *119*, 3291–6, Part 2: Ref. 13 below.

(2) Belousov, B. P. *In Oscillations and Traveling Waves in Chemical Systems;*, Field, R. J., Burger, M.,. Eds.; Wiley-Interscience, New York, 1985, pp 605−13.

(3) Zhabotinsky, A. M. *Biofizika* **1964**, *9*, 306–311.

(4) Zhabotinsky, A. *Dokl. Akad. Nauk. SSSR* **1964**, *157*, 392–395.

(5) Field, R. J. ; Kőrös, E. ; Noyes, R. M. *J. Am. Chem. Soc.* **1972**, *94*, 8649–64.

(6) Field, R. J.; Noyes, R. M. *J. Chem. Phys.* **1974**, *60*, 1877–84.

(7) Scott, S. K. *Oscillations, Waves and Chaos in Chemical Kinetics* Oxford University Press Inc. New York, 1994.

(8) Shakashiri, B. Z. *Chemical Demonstrations;* University of Wisconsin Press Madison, 1985; Vol. 2.

(9) Hastings, H. M.; Field, R. J.; Sobel, S. G. *J. Chem. Phys.* **2003**, *119*, 3291–96.

(10) Baer, S. M.; Erneux, T.; Rinzel, J. *SIAM J. Appl. Math.* **1989**, *49*, 55–71.

(11) Sobel, S. G.; Hastings, H. M.;.; Field, R. J. *J. Phys. Chem. A* **2006**, *110*, 5–7.

(12) Noyes, R. M. *J. Am. Chem. Soc.* **1980**, *102*, 4644–9.

(13) Hegedús, L.; Wittman, M.; Noszticzius, Z.; Sirimungkala, A.; Försterling, H.-D.; Field, R. J. *Disc Far. Soc.* **2002**, *120*, 21–38.

(14) Weast, R. C. (ed.); *Handbook of Chemistry and Physics 56 th Ed.*, CRC Press, Cleveland, OH, 1975, pp D141−2.

(15) Sirimungkala, A.; Försterling; H, D.; Dlask, V.; Field, R. J. *J. Phys. Chem. A* **1999**, *103*, 1038–43.

(16) Hansen, E. W.; Ruoff, P. *J. Phys. Chem.* **1988**, *92*, 2641–45.

(17) Jwo, J.-J.; Noyes, R. M. *J. Am. Chem. Soc.* **1975**, *97*, 5422–31.

(18) Kuhnert, L.; Pohlmann, L.; Krug, H.-J. *Physica D* **1988**, *29*, 416–20.

(19) Ruoff, P.; Noyes, R. M. *J. Phys. Chem.* **1989**, *93*, 7394–98.

(20) Krug, H.-J.; Pohlmann, L.; Kuhnertt, L. *J. Phys. Chem.* **1990**, *94*, 4862–66.

(21) Treindl, L. ; Ruoff, P. ; Kvernberg, P. O. *J. Phys. Chem. A* **1997**, *101*, 4606–12.

(22) Steinbock, O.; Hamik, C. T.; Steinbock, B. *J. Phys. Chem. A* **2000**, *104*, 6411–15.

(23) Hansen, E. W.; Ruoff, P. *J. Phys. Chem.* **1989**, *93*, 2696–2704.

JP8019073